Oxidative dehydrogenation of alcohols on gold

Mastroianni, Luca; Weckman, Timo; Eränen, Kari; Russo, Vincenzo; Murzin, Dmitry Yu; Honkala, Karoliina; Salmi, Tapio

Published in:
Journal of Catalysis

DOI:
10.1016/j.jcat.2023.06.017

Published: 01/09/2023

Document Version
Final published version

Document License
CC BY

Journal of Catalysis 425 (2023) 233–244

Contents lists available at ScienceDirect

Journal of Catalysis

journal homepage: www.elsevier.com/locate/jcat

Oxidative dehydrogenation of alcohols on gold: An experimental and computational study on the role of water and the alcohol chain length

Luca Mastroianni [a,c], Timo Weckman [b], Kari Eränen [a], Vincenzo Russo [a,c], Dmitry Yu. Murzin [a,*], Karoliina Honkala [b], Tapio Salmi [a]

[a] Åbo Akademi University, Henriksgatan 2, Åbo/Turku 20500, Finland
[b] University of Jyväskylä, Finland
[c] Università degli Studi di Napoli Federico II, Via Cintia, Naples 80126, Italy

ARTICLE INFO

Article history:
Received 24 April 2023
Revised 8 June 2023
Accepted 12 June 2023
Available online 16 June 2023

ABSTRACT

The oxidative dehydrogenation of primary alcohols promoted by gold nanoparticles was investigated from an experimental and computational viewpoint to derive a plausible reaction mechanism and to understand the role of water and alcohol chain length in the elementary steps. The influence of water in reaction kinetics and product distribution was determined in a laboratory-scale microreactor adding water to the reaction mixture in different amounts. DFT calculations revealed that the presence of water on the catalyst surface is beneficial to assist the key step in alcohol oxidation i.e., oxygen activation by protonation. The calculations were performed for primary alcohols ranging from methanol to butanol to understand the role of the alkyl chain length on the catalytic activity and to clarify experimental observations. General conclusions were drawn on the influence of temperature on product distribution when employing a typical support material for gold nanoparticles, Al_2O_3. The combination of experiments and theory has been useful to improve the knowledge of alcohol oxidation promoted by gold.

1. Introduction

Selective oxidation of primary alcohols to corresponding aldehydes plays a pivotal role in the modern chemical industry [1]. Alcohols, which are widely obtained from the bio-based raw materials, can significantly contribute to a decrease of the dependence from fossil resources. In selective oxidation reactions, traditionally employed chromium based stoichiometric reagents might be replaced by molecular oxygen, thus improving the atom efficiency of the oxidation process [2].

Oxide-supported gold nanoparticles have emerged as promising heterogeneous catalysts among several alternatives due to their high activity and selectivity towards the carbonyl group. Although Fokin [3] reported catalytic activity of gold more than one hundred years ago, the scientific community for many decades did not further actively pursue potential applications of gold catalysts. The breakthroughs of Haruta [4,5] and Hutchings [6], who employed gold nanoparticles as active materials in low-temperature catalytic oxidation of gold and hydrochlorination of acetylene respectively, dramatically changed this scenario [7]. The catalytic properties of gold are observed only at the nanoscale disappearing in a larger scale [8].

Concerning the structure sensitivity of gold in alcohol selective oxidation, conflicting results were reported in the literature [9]; therefore, experimental and computational studies have been carried out to comprehend the structure- and size-dependent reactivity of gold catalysis in alcohol oxidative dehydrogenation [10–12]. Atomic level understanding of the reaction mechanism is crucial to elucidate experimental results, thus optimizing the catalytic performance of Au in alcohol oxidation. Lateral interactions between the reactants and the products on the catalytic surface might affect reaction energetics, having a significant impact on the oxidation reaction. Therefore, evaluation and computation of adsorption and reaction steps is fundamental to improve understanding of a catalytic process leading to eventual catalyst optimization.

The essential step in the process of alcohol oxidation is the dissociation of molecular oxygen. Theoretical [13–15] and experimental [16] studies have shown that molecular oxygen does not chemisorb onto low-index gold surfaces. Due to weak interactions with the gold surface, the molecular oxygen retains its triplet state upon adsorption and a change in the spin state from a triplet into a singlet state is very endothermic. The density functional theory studies place the weak adsorption energy in the range of −0.1 eV while the barriers for dissociation on flat gold surfaces are well above 1 eV. When moving to higher-index surfaces [17], the ratio between the dissociation and desorption barrier decreases but

* Corresponding author.
E-mail address: dmurzin@abo.fi (D.Yu. Murzin).

https://doi.org/10.1016/j.jcat.2023.06.017
0021-9517/

remains substantial. However, it has been suggested [9] that the O_2 could be activated by the co-adsorption of O_2 and an alcohol. Moreover, it has been stated that the adsorption of O_2 is endothermic as the spin state of the molecule converts from the gas-phase triplet state to a singlet state [18]. However, in the singlet state the O_2 molecule can facilitate the dissociation of the methanol O-H bond with a barrier of 0.91 eV. Combining these two steps gives an overall barrier of 1.52 eV, lower than the dissociation of O_2 on the flat Au (2.44 eV) or the cleaving of the O-H bond from alcohol in the absence of O_2 (2.18 eV). While methanol was used as the reference alcohol for the computational studies, more recently, the same concepts were extended to ethanol oxidation [9].

Alcohol oxidation promoted by gold has been extensively studied from the experimental viewpoint. Xu *et al.* [19] investigated the oxygen assisted cross-coupling of MeOH, EtOH and BuOH on oxygen covered Au (111). The reaction has been proposed to begin with the cleavage of the alcohol O-H bond to form a metal-alkoxyl group, followed by a rate-determining β -hydride elimination to produce a carbonylic product. Recently, reaction kinetics and product distribution in the oxidation of primary alcohols promoted by Au/Al_2O_3 catalyst was investigated in a microreactor [20]. A decline of the catalytic activity with the alkyl chain length in the C_1–C_3 range was observed, while propanol and butanol exhibited the same reactivity in selective oxidation.

Apart from the reacting molecules, water has been proposed to play a prominent part in the in the activation of molecular oxygen in oxidation processes [21–23]. While water is not fed in the reactor, it is unavoidably formed as a stoichiometric product during the process and may be present in substantial amounts in the reaction mixture. Moreover, steam and moisture can be also a part of the feed gas. The impact of water in oxidation is well known for several oxidation processes, such as propene epoxidation [24–26] and CO oxidation [27–30]. For these processes, it is considered that water facilitates O_2 adsorption, thus activating it for the catalytic process. Water-assisted protonation of oxygen on a gold catalyst has been previously investigated computationally [18]. Obtained DFT results indicated formation of a reactive OOH intermediate via the protonation of a molecular oxygen and the presence of two water molecules can make the protonation process even more facile.

The present work investigates the effect of water in promoting alcohol oxidation, both experimentally and computationally. Experiments in which water was added to the gas feed in different amounts were carried out in a microreactor to reveal the impact of water and the reaction orders in ethanol oxidation, chosen as the reference reaction for alcohol oxidation. Density Functional Theory (DFT) calculations were performed to explore the reaction mechanism theoretically and compare the calculations with experimental data.

The oxidation pathways of methanol, ethanol, propanol and butanol were investigated from a computational viewpoint on Au (111) surface in the presence and absence of water to understand its role in elementary steps, thus proposing a plausible reaction mechanism for alcohol oxidation promoted by gold. Co-adsorption effects were revealed to be of fundamental importance in the explanation of the experimental evidence, particularly for the role of water and alcohol chain length in the oxidation process. The combinations of DFT and experiments enabled to unravel mechanistic aspects and impact of water in alcohol oxidation promoted by alumina-supported gold nanoparticles.

2. Experiments and methods

2.1. Catalytic experiments

The kinetic experiments were conducted in a gas-phase microreactor coated with Au/ γ -Al_2O_3 catalyst. Gold nanoparticles were dispersed on γ-alumina (UOP, A-201) support by using the direct ion exchange (DIE) method. An aqueous solution containing $HAuCl_4$ precursor was mixed with γ-Al_2O_3 and heated up at 70 °C. Ammonia was used as the washing agent prior to calcination. Additional information about the catalyst preparation is available in the related work of Simakova et al. [31]. The gold loading was 2 wt%, while the average particle size was 5 nm. Additional details about physico-chemical properties of the employed catalyst can be found in ref. [20].

The slurry-based method was employed to coat the microreactor channels [20]. Au/γ-Al_2O_3 particles were grinded and sieved with a 32 μm mesh sieve. Then, a 5 wt% Au/ γ -Al_2O_3 aqueous slurry was prepared mixing the catalyst with distilled water and adjusting the pH to 9.2 with an ammonium-hydroxide (32 %, Merck) solution. The slurry was kept under active stirring for 4 h at 50 °C and subsequently at room temperature for four days. The rotation speed was set to the value of 500 rpm.

The obtained slurry was used to deposit the catalyst onto the reactor microplates with a Finnpipette. The platelets were thermally pretreated at 750 °C in the presence of air to create an oxide layer, which increased the catalyst adhesiveness to the surface of the microreactor channels. After coating, the microplates were dried and finally calcined at 300 °C for 3 h.

The microreactor was purchased from Institut für Mikrotechnik Mainz GmbH (IMM), including ten stainless-steel microplates with nine channels each (Fig. 1a).

The mixing of the gas-phase reactant and the inert carrier (He) was guaranteed by ten mixing plates located in front of the catalytic zone. The system was heated up to the desired temperature by employing two cylindrical cartridges, which was monitored by a PID controller (CalControls 9500P) and measured with a thermocouple. A schematic process-flow diagram is displayed in Fig. 2.

Various ethanol–water solutions were prepared and fed to the microreactor device to investigate the influence of water on ethanol conversion and the product distribution. The total amount of water in the feed was varied from 0 to 20 mol % with respect to the ethanol concentration. The total volumetric flow rate was fixed at 50 mL min^{-1} while the reaction temperature was 250 °C. The ethanol partial pressure in the feed and the oxygen-to-ethanol molar ratio were 0.21 atm and 2, respectively. During the catalytic experiments, stability tests were conducted repeating a reference experiment after changes of the process conditions to detect possible deactivation.

2.2. Computational details

Density functional theory (DFT) as implemented in GPAW 21.1.0 [33] was employed to conduct the calculations. The Kohn–Sham equations were solved using a plane-wave basis set with a cutoff of 600 eV. The exchange–correlation functional was approximated using the BEEF-vdW functional [34], which combines the generalized gradient approximation with a Langreth–Lundqvist-type van der Waals -functional [35]. The lattice constant of bulk gold was optimized to 4.23 Å. The calculations on the Au (111) surface were performed using a 3×3 non-orthogonal surface unit cell with a five-layers thick slab, where the bottom two layers were constrained to remain in the bulk positions.

The surface slab was periodic in the *xy*-plane and the k-point sampling for the surface calculations was done using a $3 \times 3 \times 1$ grid. The structure optimization was carried out using the BFGS algorithm until the forces were below the threshold of 0.05 eV/Å. Transition states were investigated using the nudged elastic band (NEB) [36,37] method as implemented in the Atomic Simulation Environment (ASE) version 3.21.0 [38] with 10 images for each pathway. The initial guess for the NEB calculations were obtained from a linear interpolation between an initial guess of the transition state and the initial and final states. The pathways were optimized using the FIRE optimizer [39].

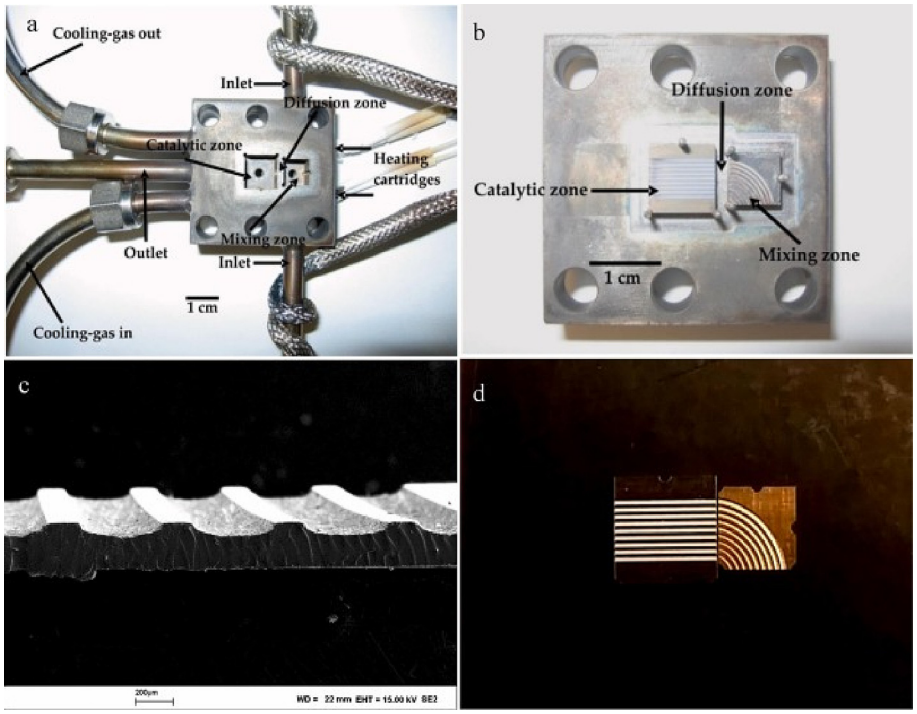

Fig. 1. A) general view of the microreactor body b) housing of the mixing and catalytic plates c) microplates cross-section d) mixing unit and a microplate. (from [32]).

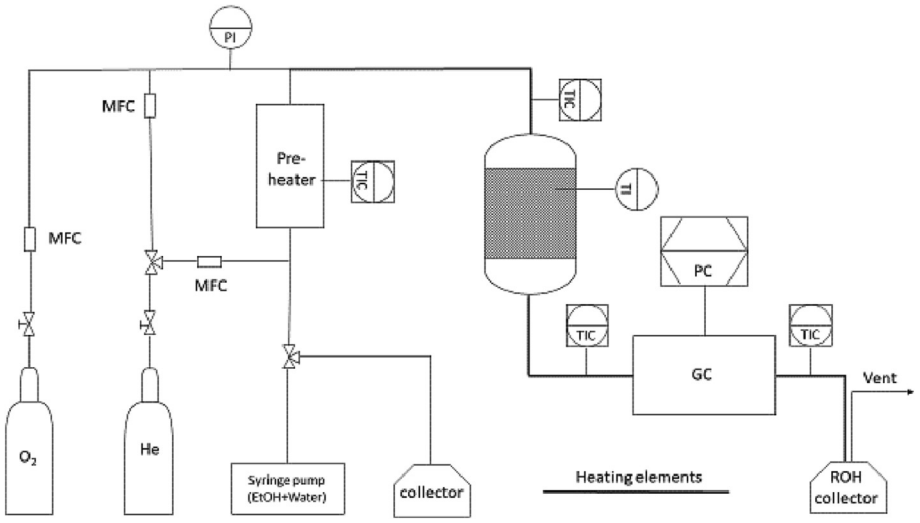

Fig. 2. Schematic process flow diagram of the microreactor system (modified from [20]).

The adsorption energies for different molecules were computed as the difference between the total energy of the adsorbed configuration $E_{surf+mol}$ and the clean surface E_{surf} and the molecule in the gas-phase E_{mol},

$$E_{ads} = E_{surf+mol} - E_{surf} - E_{mol} \quad (1)$$

The adsorption of molecular oxygen onto gold is endothermic due to a conversion of the O_2 spin state from a triplet to a singlet. Co-adsorption with alcohol and water may stabilize O_2 adsorption. To quantify this effect, water—alcohol co-adsorption structures with and without O_2, shown for methanol in Eq (2), should be considered.

$$3O_2^* + (MeOH + H_2O)^* \Longleftrightarrow (MeOH + H_2O + {}^1O_2^*)^* \quad (2)$$

The energy change associated with this process can be computed according to Eq. (3) for any alcohol molecule.

$$\Delta\Delta E = E_{co-ads,\ with\ O_2} - E_{co-ads,\ without\ O_2} - E_{ads,\ O_2} \quad (3)$$

A positive $\Delta\Delta E$ value indicates that molecules adsorbed infinitely far away from each other are more stable than when they are co-adsorbed, whereas a negative value indicate stabilization of co-adsorbed structure compared to the individual molecules.

3. Results and discussion

3.1. Catalytic experiment results

3.1.1. Reaction network

Based on the experimental observations and obtained products the reaction network comprises three parallel reactions. Together with ethanol selective oxidation, etherification and alkene formation proceeded simultaneously on the catalyst surface of gold

and the support (Fig. 3). Namely, the oxidative dehydrogenation of ethanol is promoted by gold while the side reactions occur on alumina [40,41]. Thermodynamic calculations highlighted that the condensation of two molecules of ethanol to give diethyl ether is strongly limited by the equilibrium [20].

3.1.2. Stability test

The stability of the catalytic coating was tested repeating a reference experiment periodically during kinetic investigations. As shown in Fig. 4 the catalyst was stable over ca. 200 h of operation as neither catalytic activity nor the product distribution was changing with time on stream. Therefore, the kinetic results were not affected by any catalyst deactivation.

3.1.3. Effect of water in ethanol oxidation

Selectivity toward acetaldehyde is greatly enhanced by the presence of water (Fig. 5). As the etherification reaction is limited by the equilibrium, an increase in selectivity when adding water was somehow expected. Water addition enhances the backward reaction, and the etherification reaction rate becomes lower.

As the ether formation reaction is slower in the presence of water, ethanol conversion was expected to decrease with the water content in the feed, because of the lower ethanol consumption. Fig. 6 demonstrated that this was not the case and, on the contrary, there was a positive impact of water on ethanol conversion. Regarding alcohol oxidation to aldehydes, a similar promoting effect was previously observed in the liquid-phase oxidation of benzyl alcohol to benzaldehyde [42].

The apparent reaction order with respect to water was estimated using the following empirical equation

$$X_{EtOH} = \alpha + \beta C_{H2O}^{n} \quad (4)$$

where X_{EtOH} is conversion of ethanol and α is a term, which takes into account catalytic activity in the absence of water. Non-linear regression analysis allowed estimation of the exponent n, which was found to be 1.6. Thus, a clear impact of water in the oxidative dehydration reaction could be established pointing out that a more detailed mechanistic insight into the oxidation pathways in the presence of water is necessary.

3.2. DFT analysis

3.2.1. Reaction scheme for oxidative dehydrogenation on Au (111)

The mechanistic aspects of alcohol oxidation on gold have been studied both experimentally and theoretically [19,43–46]. From studies conducted on Au(111) surfaces pre-covered with atomic oxygen [43–46], it has been established that the dehydrogenation of primary alcohols occurs in two-steps, beginning with the cleavage of the O–H bond of the alcohol, followed by the rate-limiting step, the elimination of the β-hydrogen.

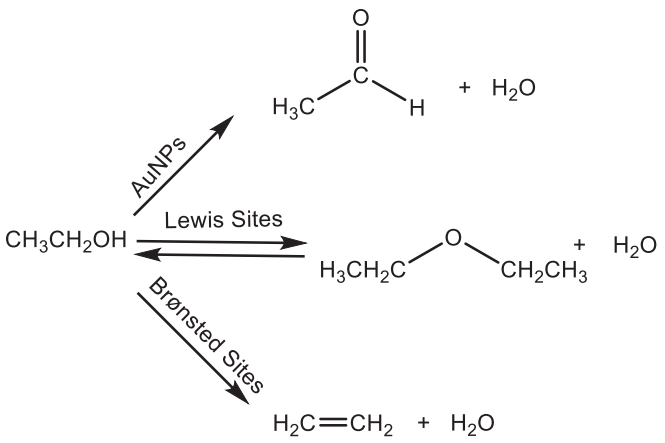

Fig. 3. Reaction network for ethanol oxidation promoted by Au/Al_2O_3.

However, it is well known that gold is unable to dissociate molecular oxygen. The barrier for dissociation is high and the interaction between the surface and O_2 is weak overall. Therefore, for a continuous process, the main question is what is the mechanism by which the molecular oxygen is dissociates on the gold surface. Chang *et al.* [18] suggested that oxygen co-adsorption with alcohols and water could activate the oxygen via protonation, leading to an intermediate species OOH, which would then be able to dissociate on the gold surface. The protonation of O_2 would promote the dissociation of the O—O bond, resulting in active oxidizing agents (O and OH) on the surface. The co-adsorption is needed to stabilize molecular oxygen on the gold surface. Upon adsorption, the O_2 can convert from a triplet state to a singlet state, which is a highly endothermic process [18]. Compared with −0.25 eV adsorption of O_2 and H_2O separately, there is a 0.42 eV increase in energy due to the change in the spin state in the case of their co-adsorption. Adding another water molecule makes the co-adsorption exothermic with −0.17 eV, compared to −0.41 eV for the isolated molecules.

The oxidative dehydrogenation via the formation of OOH intermediate on gold can be summed up as a reaction network following the equations (5) to (15). In the network, several possible pathways for protonation of O_2 have been considered.

O_2 protonation

$$H_2O* + O_2* \rightarrow OH* + OOH* \quad (5)$$

$$2H_2O* + O_2* \rightarrow H_2O* + OH* + OOH* \quad (6)$$

$$2RCH_2OH* + O_2* \rightarrow RCH_2OH* + RCH_2O* + OOH* \quad (7)$$

$$H_2O* + RCH_2OH* + O_2* \rightarrow RCH_2O* + H_2O* + OOH* \quad (8)$$

$$2H_2O* + RCH_2OH* + O_2* \rightarrow RCH_2O* + 2H_2O* + OOH* \quad (9)$$

O_2 dissociation

(6) $$OOH* \rightarrow O* + OH* \quad (10)$$

OH cleavage

$$RCH_2OH* + OH* \rightarrow RCH_2O* + H_2O* \quad (11)$$

$$RCH_2OH* + OOH* \rightarrow RCH_2O* + H_2O_2* \quad (12)$$

β-elimination

$$RCH_2O* + O* \rightarrow RCHO + OH* \quad (13)$$

$$RCH_2O* + OH* \rightarrow RCHO + H_2O* \quad (14)$$

$$RCH_2O* + OOH* \rightarrow RCHO + H_2O_2* \quad (15)$$

In this work, different co-adsorption complexes consisting of alcohols, water and molecular oxygen have been investigated and the subsequent protonation of O_2 within these complexes (Eqs. (5)–(9)) as well as the dissociation of the resulting hydroperoxyl (Eq. (10)). In addition, the two-step alcohol dehydrogenation pathways, consisting of the O–H cleavage (Eqs. (10)–(11) and β-elimination (Eqs. (12)–(14)) with different oxidizing agents (O*, OH*, OOH*) have been studied. Reaction networks are established for the four smallest primary alcohols, methanol, ethanol, propanol, and butanol.

3.2.2. Adsorption of alcohols, O_2 and H_2O

All the alcohol molecules bind to the Au (111) surface via the oxygen atom, preferably on the Au-top site, see Fig. 7a. The

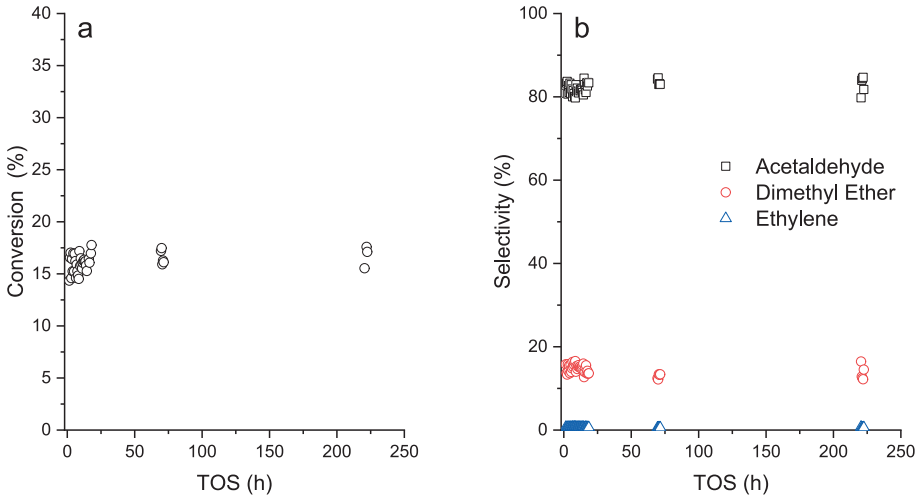

Fig. 4. A) oxidative dehydrogenation over au/al$_2$O$_3$ as a function of TOS: a) ethanol conversion b) selectivity. Experimental conditions: T = 250 °C, p_{EtOH} = 0.21 atm. The oxygen – to – ethanol molar ratio was 2 and no water was fed in the reactor.

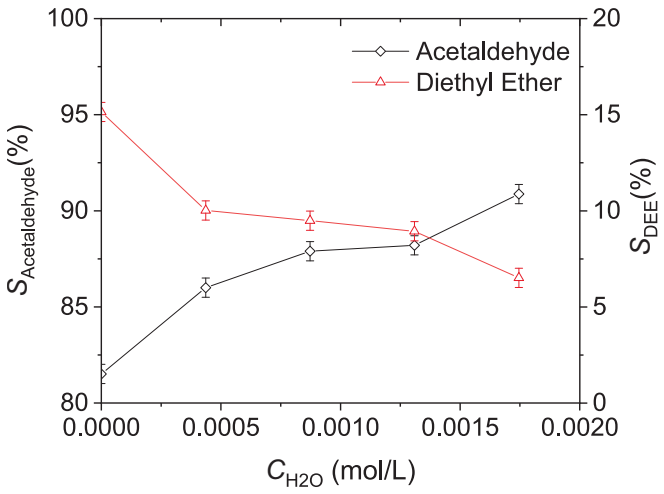

Fig. 5. Effect of water on selectivity to acetaldehyde and diethyl ether.

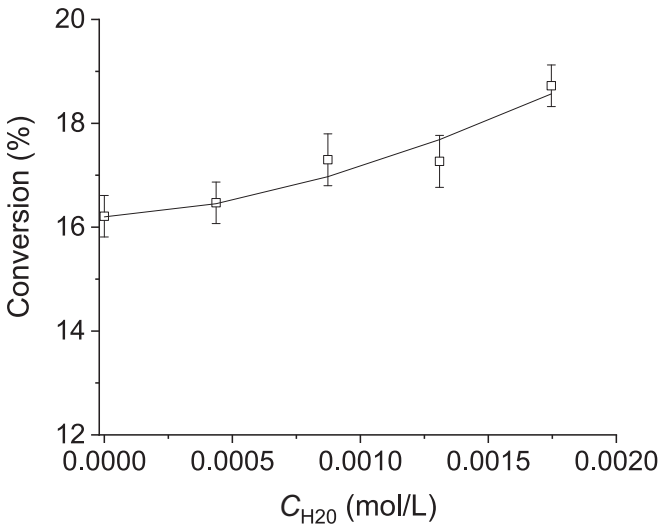

Fig. 6. Effect of water in ethanol oxidation on ethanol conversion.

carbon-chain tends to lie along the surface due to the attractive van der Waals (vdW) interactions between the chain and the surface [47]. Subsequently, the adsorption energy of the alcohols increases linearly with the increasing chain length from −24.0 kJ mol^{-1} for methanol to −38.0 kJ mol^{-1} to butanol, reflecting the growing attraction between the surface and the carbon chain. The Au—O bond lengths are rather similar among the studied alcohols and range from 2.85 Å for methanol to 2.92 Å for ethanol.

Table 1 compares the calculated and measured alcohol adsorption energies. The experimental adsorption energy values are more exothermic by ∼16 kJ mol^{-1} compared to the computed ones but the trends for adsorption energies are similar. In agreement with the literature [9] our calculations show that molecular oxygen adsorbs weakly on Au (111) with the adsorption energy of only −8.7 kJ mol^{-1}, preferring a parallel orientation over the bridge site and retaining its gas-phase triplet state. This indicates that oxygen is not activated and the interaction with the surface is weak physisorption. When adsorbing in a singlet state, the adsorption is endothermic by 68.5 kJ mol^{-1}.

Co-adsorption of O_2 with alcohol and/or water molecules were explored, and Table 2 summarizes all the computed co-adsorption energies as well as the protonation barriers within the co-adsorption structures. To quantify the extent to which co-adsorption compensates for the change in the O_2 spin state, ΔΔE was determined according to Eq. (3), which compares the formation energy of a co-adsorption structure with and without the molecular oxygen. The co-adsorption energies are listed in Table 2. Fig. 7 shows atomic structures for the selected co-adsorption configurations.

As discussed above, an isolated molecular oxygen retains its triplet state on gold surface and the conversion of a triplet state of the molecular oxygen into a singlet state is an endothermic process. Co-adsorption with a single alcohol or water molecule does not sufficiently stabilize O_2 on the surface. While the co-adsorption energy with propanol and butanol is negative, the overall co-adsorption energy is still weak and co-adsorption structures with more co-adsorbates were explored.

With two co-adsorbates, the co-adsorption energy is negative for all alcohols. For the alcohol—O_2—alcohol complex ΔΔE is about 52 kJ mol^{-1} while for an alcohol—O_2—water complex ΔΔE is only about 35 kJ mol^{-1}. The lower ΔΔE value means that the thermodynamic barrier to form a co-adsorption structure is lower for the water-containing complex. The thermodynamically most stable

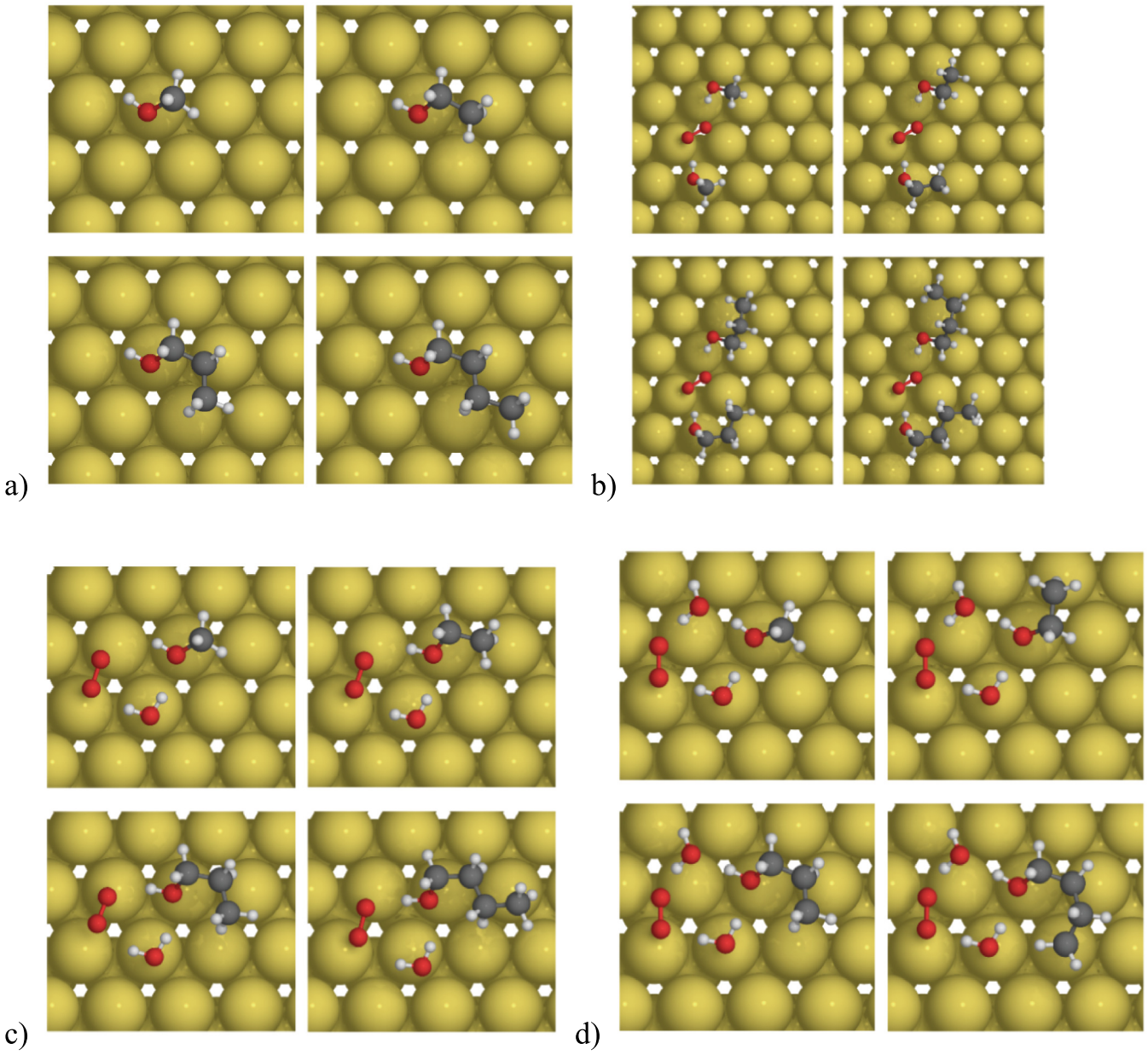

Fig. 7. Adsorption structures for a) different alcohols b) alcohol-alcohol-oxygen and c) alcohol-oxygen-water and d) alcohol-oxygen-water-water.

co-adsorption structure was obtained by adding an additional water molecule to the alcohol—water—O_2-complex. The stabilizing hydrogen bonds between the adsorbed species lead to a ΔΔE of only 20 kJ mol^{-1}, a significantly lower formation barrier for the cluster than in the previous cases.

Table 1
Adsorption energies (eV) for alcohol, water, and oxygen molecules on Au (111)*.

Substrate	Adsorption energy [kJ/mol]	Experimental[kJ/mol]
MeOH	−24.0	−38.6 [43]
EtOH	−27.0	−45.3 [44]
PrOH	−32.9	−49.2 [45]
BuOH**	−38.0	−51.1 [46]
H_2O	−15.5	
O_2	−8.7	

* Numerical values for the experimental results for monolayer coverage are taken from ref [46]. The calculated values are computed at low coverage (one alcohol molecule in a 3 × 3 unit cell). Using two alcohols in the simulation cell, the alcohol—alcohol interactions at a higher coverage are estimated to be ca. −18 kJ mol^{-1} on average for an alcohol pair or 9 kJ mol^{-1} per alcohol.

** The experimental value was measured for 2-butanol adsorption while 1-butanol was used in calculations.

3.2.3. Protonation and dissociation of O_2

Once stabilized by a co-adsorption complex, the O_2 may be protonated by either an alcohol or a water molecule, resulting in a hydroperoxyl molecule, OOH. In co-adsorption structures with a single water molecule and one or two alcohols with O_2, the activation energy consists entirely of the thermodynamic barrier, making the final state very unstable. For these pathways, no kinetic barrier is reported. The activation energies for the protonation within the other co-adsorption structures ranges from 30 to 40 kJ mol^{-1}.

The dissociation of OOH was considered with and without co-adsorbed molecules. On the bare Au(111) surface, the isolated OOH favors the bridge site. The activation energy for the dissociation is 53 kJ mol^{-1} and the reaction energy is exothermic by

Table 2
The co-adsorption energies ($\Delta E_{co\text{-}ads}$) for different molecules, the energy difference between the co-adsorbed and isolated molecules ($\Delta\Delta E$), the activation energy for the protonation of the O_2 (E_{act}), and the reaction energy of the protonation reaction (ΔE). All values are in kJ mol^{-1}.

Configuration	$\Delta E_{co\text{-}ads}$	$\Delta\Delta E$	E_{act}	ΔE
MeOH + O_2	5.4	38.1	–	36.7
EtOH + O_2	−3.1	32.7	–	40.7
PrOH + O_2	−5.9	35.7	–	35.3
BuOH + O_2	−13.4	33.3	–	36.6
H_2O + O_2	16.7	40.9	–	35.7
2 MeOH + O_2	−17.3	56.9	–	32.0
2 EtOH + O_2	−25.0	56.6	–	27.9
2 PrOH + O_2	−39.9	48.2	–	30.4
2 BuOH + O_2	−48.9	48.4	–	31.3
2 H_2O + O_2	−16.4	42.9	39.3	34.0
O_2 + MeOH + H_2O	−29.9	35.2	42.5	39.3
O_2 + EtOH + H_2O	−34.7	35.2	41.0	36.2
O_2 + PrOH + H_2O	−38.6	35.5	42.0	33.5
O_2 + BuOH + H_2O	−45.3	35.6	41.6	36.3
O_2 + MeOH + 2H_2O	−86.8	17.4	39.0	22.2
O_2 + EtOH + 2H_2O	−90.7	21.0	38.3	22.8
O_2 + PrOH + 2H_2O	−95.5	28.8	38.9	25.2
O_2 + BuOH + 2H_2O	−94.6	23.1	42.5	29.2

*A 4 × 4 simulation cell was used for the calculations with two alcohols.

−43 kJ mol^{-1}. However, since protonation is likely to occur within a co-adsorption structure, the influence of the complex on dissociation was also addressed. Within a MeO–H_2O–OOH complex, the activation and reactions energies for OOH dissociation are 60 kJ mol^{-1} and −67 kJ mol^{-1}, respectively, and thus the presence of co-adsorbed species has a minor impact on dissociation energetics. The protonation pathways for MeOH in the co-adsorption structures are illustrated in Fig. 8.

Table 3
Activation energies [kJ mol^{-1}] for oxidation reaction with O/OH/OOH and alcohols/alkoxy species on Au(111).

	Substrate	Surface species		
		O	OH	OOH
O–H – cleavege	MeOH	–	15.7	24.7
	EtOH	–	14.9	24.6
	PrOH	–	13.2	25.7
	BuOH	–	12.2	25.6
β - elimination	MeO	45.3	75.6	93.8
	EtO	41.6	78.6	98.7
	PrO	41.2	67.3	90.2
	BuO	40.3	72.7	86.7

3.2.4. Oxidative dehydrogenation of alcohols

The protonation pathway results in multiple oxidation agents on the surface. In addition to the O* and OH* resulting from hydroperoxyl dissociation, OOH* itself can also participate in alcohol dehydrogenation. Therefore, we therefore considered the cleaving of the alcohol O–H bond by OH and OOH groups as well as the reactivity of O, OH and OOH groups on the β-elimination of the resulting alkoxy groups. The O–H bond breaking by atomic oxygen on gold has been established as a rapid process [18,43–46] and was excluded from the present work, which focuses on the rate controlling elementary steps. The computed activation energies for the O–H bond breaking and β-elimination for different alcohols and oxidation agents are collected in Table 3 and the corresponding reaction pathways for MeOH are illustrated in Figs. 9 and 10.

When the OOH group participates into the oxidative dehydrogenation of alcohols, a hydrogen peroxide molecule, H_2O_2, is pro-

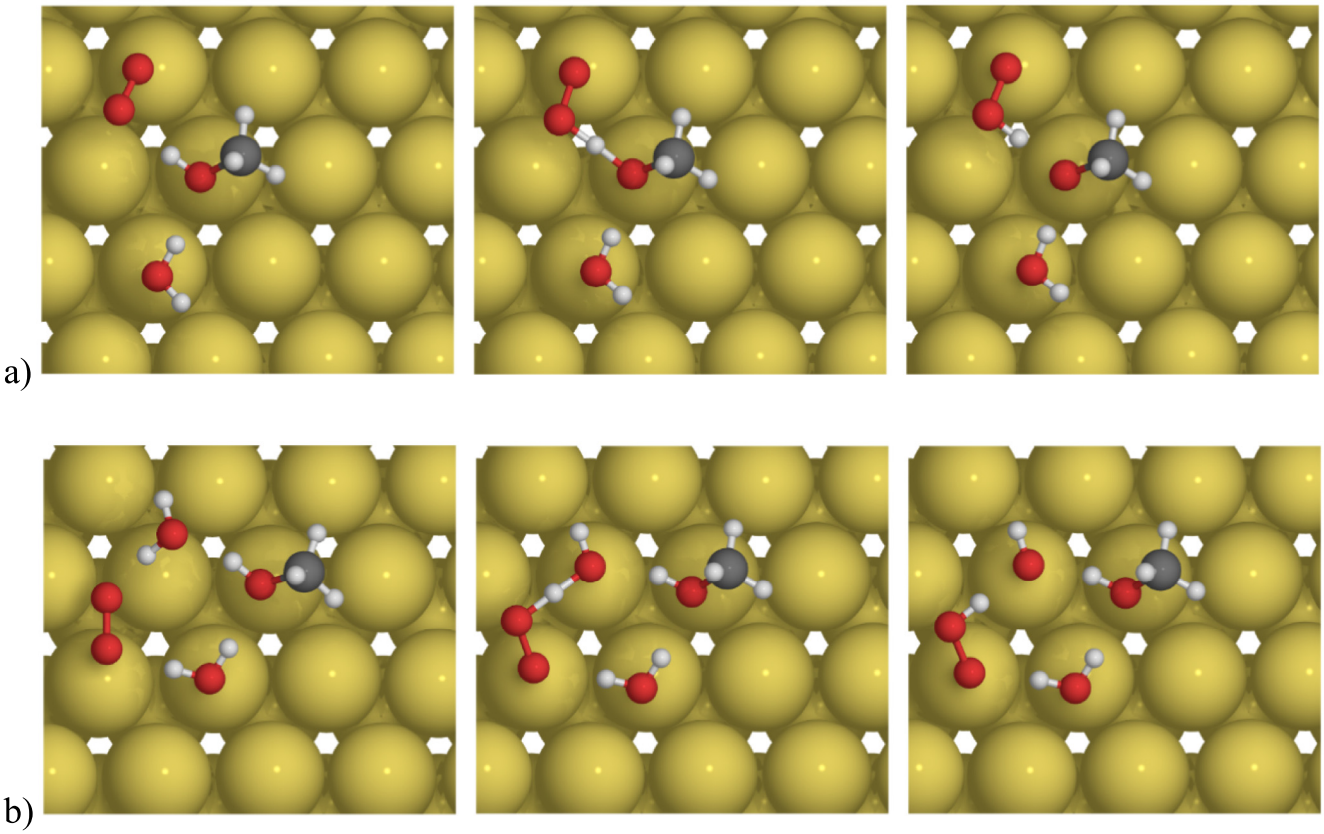

Fig. 8. The protonation pathways in the co-adsorption structures for a) MeOH-H_2O–O_2 and b) MeOH–2 H_2O–O_2 configurations. The images are, from left to right, the initial, transition and final states, respectively.

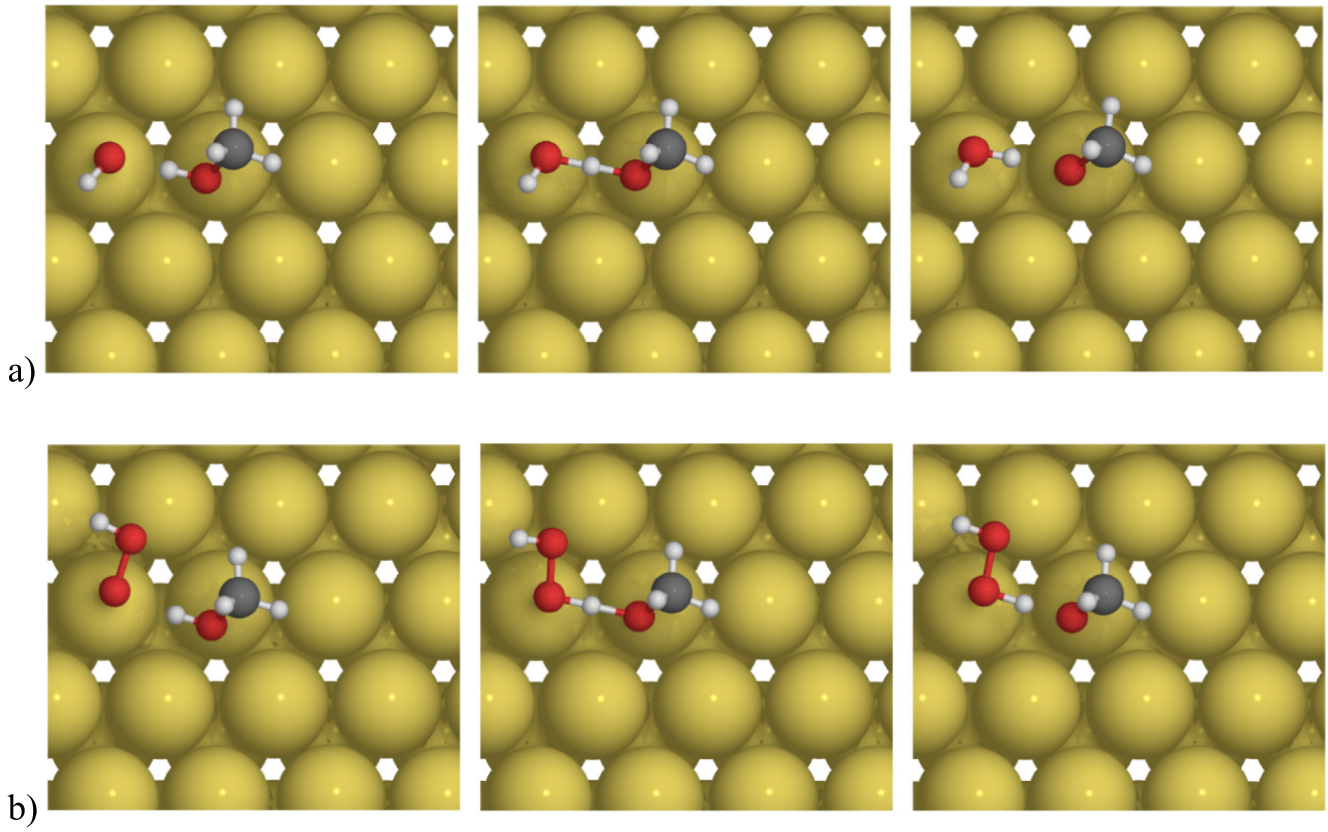

Fig. 9. The reaction pathways for cleaving the O–H-bond from MeOH by a) OH, b) OOH. The images are, from left to right, the initial, transition and final states, respectively.

duced. The activation energy for the dissociation of H_2O_2 on the gold surface is 42 kJ mol^{-1} with a reaction energy of −65 kJ mol^{-1}.

OH* and OOH* assisted breaking the alcohol O-H bond is a facile process and the activation energies range from 14 (with OH*) to 25 (with OOH*) kJ mol^{-1}. For the OH-assisted pathway, the activation energy decreases monotonically as a function of the carbon chain length in alcohol. However, this change is within the DFT error. For OOH*, the activation energies are independent of the alcohol.

In agreement with the experimental findings [19] the computed activation energies are considerably higher for the β-elimination step than for the O-H bond cleavage. For the O*, OH* and OOH* oxidized pathways, the activation energies are ∼40, ∼70 and ∼90 kJ mol^{-1}, respectively. In the case of atomic oxygen, the activation energies decrease monotonically with the carbon chain length in line with the experimental observations [19], but like the O–H bond cleavage, the change is small and within the DFT error. For OH* and OOH*, no trend is seen for the activation energies. Considering the high activation energy for the β-elimination step with OOH*, and the instability of the alkoxy-–OOH* pair discussed earlier, the β-elimination via OOH* can be deemed unfeasible.

3.2.4.1. Ether formation on alumina support. Au nanoparticles are often dispersed on γ-Al_2O_3 support, and the support may actively participate in catalytic chemistry. A reaction competing with the dehydrogenation of the alcohols is the coupling reaction resulting in ethers. The formation of ethers on alumina has been computationally studied for methanol [48,49], ethanol [50–52], and propanol [53,54]. Most studies consider a bare alumina surface, while some include surface hydroxylation [51] and even discuss the effect of surface hydroxylation on the ether formation [52], suggesting that alumina hydroxylation inhibits the ether formation.

Whatever the exact nature of the active sites, ethanol dehydration requires acid sites on the catalyst surface, contrary to oxidative dehydrogenation occurring on gold nanoparticles. Addition of gold enhanced selectivity towards acetaldehyde in comparison with the neat support [55] without improving the rate of the ether formation. This implies that gold is not involved in the latter reaction and subsequently formation of the ether on gold nanoparticles was excluded from the scope of the current work. Moreover, no formation of ethylacetate due to an esterification reaction was experimentally observed.

The alcohols tend to bind strongly onto γ-Al_2O_3 surface with the adsorption energies –124 kJ mol^{-1} for methanol [49], −124 kJ mol^{-1} for ethanol [51] and –136 kJ mol^{-1} for *i*-propanol [53]. The rate-limiting step in ether formation is the coupling between an alcohol molecule and a surface alkoxy species. This reaction is affected by surface orientation and surface hydroxylation. On bare alumina the reported barriers to form an ether range from 119 to 140 kJ mol^{-1} for MeOH [48,49], 79 to 191 kJ mol^{-1} for EtOH [50–52], and from 106 to 130 kJ mol^{-1} for *i*-PrOH [53,54].

The energetics reported in the studies discussed above are not directly comparable, as some include a van der Waals correction in the calculations [52,53] while others do not [48–51], and some study the reactions using a solvent model [48,49] while others assume the reactants to be in gaseous phase [48]. Nevertheless, a general conclusion is that while the oxide support binds alcohol species strongly, activation energies for ether formation are also high. This is the opposite for alcohol oxidation on gold where the binding of adsorbates is relatively weak and O–H bond breaking, and β-elimination have low activation energies. However, the main obstacle to alcohol oxidation on Au is O_2 dissociation. Comparison of these two catalysis processes highlights that temperature increase hinders already weak adsorption on gold and enhances

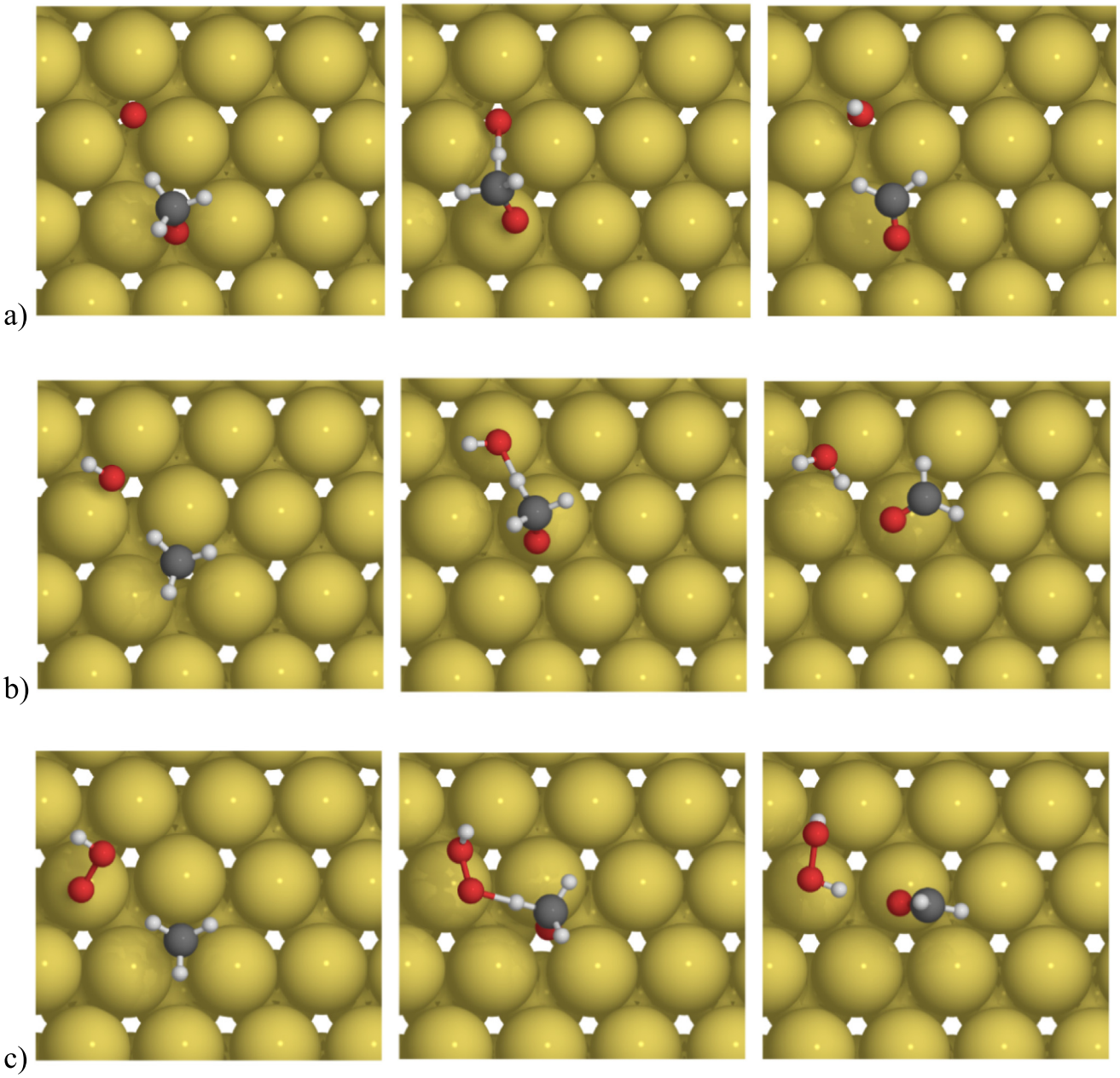

Fig. 10. The β-elimination reaction pathways for MeOH reacting with a) O, b) OH, c) OOH. The images are, from left to right, the initial, transition and final states, respectively.

ether formation on the oxide, justifying the increase in selectivity toward diethyl ether as a function of temperature observed on Au/Al_2O_3 catalyst [20].

3.2.5. Bridging computation and experimental observations

A comprehensive analysis of the dehydrogenation reaction network using DFT calculations has been presented. The co-adsorption structures with water play a crucial role in stabilizing the molecular oxygen onto the gold surface, hence promoting the oxidation process. Within these co-adsorption structures, the O_2 can be protonated into OOH, which can then dissociate, resulting in atomic oxygen and hydroxyl group on the surface. A potential energy diagram for selected methanol structures is displayed in Fig. 11.

The two-step pathway for alcohol dehydrogenation was explored for the four alcohols considered in this work. The activation energy of the first O–H cleaving step was lower than the subsequent β-elimination, in the case of each oxidizing agent (O*, OH*, OOH*) for all alcohols. This is in excellent agreement with the experimental results [19,56,57], which show that the beta-elimination is the rate-determining step. Relative differences in reactivities among the alcohols were, however, small and within the numerical error.

The main difference between the alcohols included in this work was in the increasing adsorption energy as a function of the alcohol chain length: while this can promote the chemical reaction, too high binding energies can also be detrimental for the catalytic activity. This might explain the decrease of the catalytic activity with the increasing alcohol chain length observed previously [20].

When utilizing γ-Al_2O_3 as the support material to disperse the gold nanoparticles, etherification reaction might occur on the Lewis acid sites of the support. High temperatures promote the coupling of two molecules of alcohol to give the ether; on the contrary, they inhibit the key step of oxidative dehydrogenation i.e., oxygen adsorption and activation. This is in full agreement with

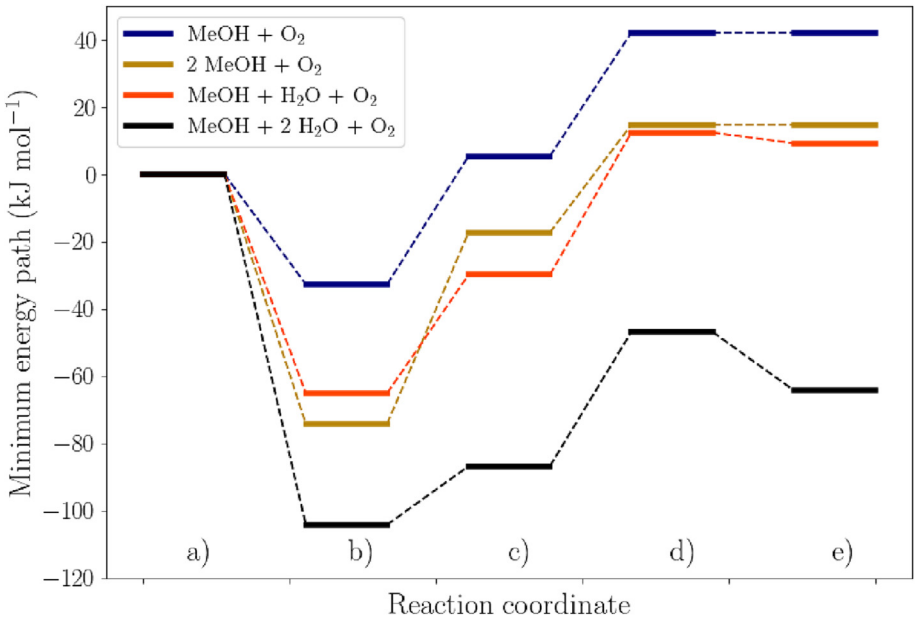

Fig. 11. Potential energy surface for different co-adsorption structures for the O_2 protonation pathway: a) The bare Au(111) surface, b) the adsorption energy of O_2 adsorbed on Au(111) separately and water and alcohol molecules forming a co-adsorption structure without O_2 (discussed in Section 2.2), c) co-adsorption energy where all the adsorbates are brought together to form a complex, d) transition state for the protonation of O_2, either by the alcohol or the water molecule, e) final state for the protonation. For the reaction pathways with one or two alcohol molecules, the protonation barrier consists entirely of the thermodynamic barrier.

the activation energies and product distributions observed experimentally for alcohol oxidation over Au/Al_2O_3 heterogeneous catalyst [20].

4. Conclusions

Computational and experimental investigations were carried out to clarify the reaction mechanism of the selective oxidation of primary alcohols promoted by Au (111) and to reveal the impact of water in key elementary steps i.e., oxygen activation and dissociation. Methanol, ethanol, 1-propanol and 1-butanol were selected as reactants for DFT calculations to explore the effect of the alkyl chain length of the primary alcohol in the oxidation reaction.

The influence of water in ethanol oxidation was experimentally investigated in a microreactor coated with Au/Al_2O_3 catalyst. Improved ethanol conversion and acetaldehyde selectivity were observed. During the experiments, stability tests were conducted to prove that the obtained experimental data were not affected by catalyst deactivation. The apparent reaction order with respect to water was 1.6, demonstrating a positive impact of water in the oxidation process.

The experimental observations were rationalized by investigating different reaction pathways with DFT, revealing that water involvement in oxygen protonation led to a more facile oxygen dissociation, thus enhancing the oxidation process. Water improves the binding energies of the reactants via the formation of hydrogen-bonding networks. The calculations are in line with the experimental data showing that oxygen dissociation becomes more energetically feasible in the presence of water and leading to enhancement of selectivity towards the aldehyde formation,

The alcohol oxidation results were compared to previous computational studies for ether formation on γ-Al_2O_3. It was concluded that higher temperatures benefit ether formation, while the oxygen activation on gold is inhibited. The computational results explain dependence of the product distribution as a function of temperature observed on $Au/\gamma—Al_2O_3$ catalyst [20].

The main trends for different alcohols were noticeable in their adsorption energies and in the activation energies for oxidation with the lowest reaction barriers being cleaving of the O-H bond by OH and β elimination of the alkoxy group by the atomic oxygen. The differences between reaction barriers lie, however, within the numerical errors of DFT calculations, thus a care should be taken regarding the mechanistic interpretation of the calculations.

Overall, a combination of DFT-calculations and experiments adopted in this work improved the atomic-level understanding especially on the role of water in the oxidative dehydrogenation of primary alcohols, forming a solid basis in developing improved alcohol oxidation processes.

Declaration of Competing Interest

The authors declare that they have no known competing financial interests or personal relationships that could have appeared to influence the work reported in this paper.

Acknowledgements

The electronic structure calculations were made possible by computational resources provided by the CSC --- IT Center for Science, Espoo, Finland (https://www.csc.fi/en/) and computer capacity from the Finnish Grid and Cloud Infrastructure (urn:nbn:fi:research-infras-2016072533). TW and KH acknowledge Jane and Aatos Erkko Foundation for the funding for the LACOR project. Antoine Meunier is acknowledged for the experimental support.

Appendix A. Supplementary materials

The computational structure files for the most stable adsorption geometries and transition states are available through the Etsin fairdata service at https://etsin.fairdata.fi/dataset/1981fe70-242b-4016-a0db-678886c0d808.

Data availability

Data will be made available on request.

References

[1] R.A. Sheldon, I.W.C.E. Arends, G.J. Brink, A. Dijksman, Green, catalytic oxidations of alcohols, Acc. Chem. Res. 35 (2002) 774–781.
[2] A.S. Sharma, H. Kaur, D. Shah, Selective oxidation of alcohols by supported gold nanoparticles: recent advances, RSC Adv. 34 (2016) 28688–28727.
[3] R.L. Augustine, Whither Goest Thou, Catalysis, Catal. Lett. 146 (2016) 2393–2416.
[4] M. Haruta, T. Susumu, T. Kobayashi, H. Kageyama, M.J. Genet, B. Delmon, Low-temperature oxidation of CO over gold supported on TiO_2, α-Fe_2O_3, and Co_3O_4, J. Catal. 144 (1993) 175–192.
[5] M. Haruta, T. Kobayashi, H. Sano, N. Yamada, Novel gold catalysts for the oxidation of carbon monoxide at a temperature far below 0 °C, Chem. Lett. 16 (1987) 405–408.
[6] G.J. Hutchings, Catalysis: A golden future, Gold. Bull. 29 (1996) 123–130.
[7] T. Tabakova, Recent advances in design of gold-based catalysts for H_2 clean-up reactions, Front. Chem. 7 (2019).
[8] A. Corma, H. Garcia, Supported gold nanoparticles as catalysts for organic reactions, Chem. Soc. Rev. 37 (2008) 2096–2126.
[9] E. Behravesh, M.M. Melander, J. Wärnå, T. Salmi, K. Honkala, D.Y. Murzin, Oxidative dehydrogenation of ethanol on gold: Combination of kinetic experiments and computation approach to unravel the reaction mechanism, J. Catal. 394 (2021) 193–205.
[10] M. Boronat, A. Corma, F. Illas, J. Radilla, T. Ródenas, M.J. Sabater, Mechanism of selective alcohol oxidation to aldehydes on gold catalysts: Influence of surface roughness on reactivity, J. Catal. 278 (2011) 50–58.
[11] A. Quintanilla, V.C.L. Butselaar-Orthlieb, C. Kwakernaak, W.G. Sloof, M.T. Kreutzer, F. Kaptejin, Weakly bound capping agents on gold nanoparticles in catalysis: Surface poison?, J Catal. 271 (2010) 104–114.
[12] Y. Guan, E.J.M. Hensen, Ethanol dehydrogenation by gold catalysts: The effect of the gold particle size and the presence of oxygen, Appl. Catal. A Gen. 361 (2009) 49–56.
[13] G. Mills, M.S. Gordon, H. Metiu, Oxygen adsorption on Au clusters and a rough Au (111) surface: The role of surface flatness, electron confinement, excess electrons, and band gap, J. Chem. Phys. 118 (2003) 4198–4205.
[14] H. Liu, Y. Liu, Y. Li, Z. Tang, H. Jiang, Metal–Organic Framework supported gold nanoparticles as a highly active heterogeneous catalyst for aerobic oxidation of alcohols, J. Chem. Phys. C 114 (2010) 13362–13369.
[15] Z.P. Liu, P. Hu, A. Alavi, Catalytic role of gold in gold-based catalysts: A density functional theory study on the CO oxidation on gold, J. Am. Chem. Soc. 124 (2002) 14770–14779.
[16] G.C. Bond, D.T. Thompson, Catal. Rev. Sci. Eng. 41 (1999) 319–388.
[17] G. Tomaschun, W. Dononelli, Y. Li, M. Bäumer, T. Klüner, L. Moskaleva, Methanol oxidation on the Au (3 1 0) surface: A theoretical study, J. Catal. 364 (2018) 216–227.
[18] C.R. Chang, X.F. Yang, B. Long, J. Li, A Water-promoted mechanism of alcohol oxidation on a Au (111) surface: understanding the catalytic behavior of bulk gold, ACS Catal. 3 (2013) 1693–1699.
[19] B. Xu, R.J. Madix, C.M. Friend, Achieving optimum selectivity in oxygen assisted alcohol cross-coupling on gold, J. Am. Chem. Soc. 132 (2010) 16571–16580.
[20] L. Mastroianni, Z. Vajglová, K. Eränen, M. Peurla, M. di Serio, D.Y. Murzin, V. Russo, T. Salmi, Microreactor technology in experimental and modelling study of alcohol oxidation on nanogold, Chem. Eng. Sci. 260 (2022).
[21] U. Landman, B. Yoon, C. Zhang, U. Heiz, M. Arenz, Factors in gold nanocatalysis: oxidation of CO in the non-scalable size regime, Top. Catal. 44 (2007) 145–158.
[22] S. Alayoglu, G.A. Somorjai, Nanocatalysis II: In situ surface probes of nano-catalysts and correlative structure–reactivity studies, Catal. Lett. 145 (2015) 249–271.
[23] C. Shang, Z.P. Liu, Origin and activity of gold nanoparticles as aerobic oxidation catalysts in aqueous solution, J. Am. Chem. Soc. 133 (2011) 9938–9947.
[24] J. Huang, T. Akita, J. Faye, T. Fujitani, T. Takei, M. Haruta, Propene epoxidation with dioxygen catalyzed by gold clusters, Angew. Chem. Int. Ed. 48 (2009) 7862–7866.
[25] S. Kanungo, Y. Su, M.F. Neira D'Angelo, J.C. Schouten, E.J.M. Hensen, Epoxidation of propene using Au/TiO_2: on the difference between H_2 and CO as a co-reactant, Catal. Sci. Technol. 7 (2017) 2252–2261.
[26] S. Lee, L.M. Molina, M.J. López, J.A. Alonso, B. Hammer, B. Lee, S. Seifert, R.E. Winans, J.W. Elam, M.J. Pellin, S. Vajda, Selective propene epoxidation on immobilized Au_{6-10} clusters: The effect of hydrogen and water on activity and selectivity, Angew. Chem. Int. Ed. 48 (2009) 1467–1471.
[27] Q. Fu, S. Kudriavtseva, H. Saltsburg, M. Flytzani-Stephanopoulos, Gold–ceria catalysts for low-temperature water-gas shift reaction, J. Chem. Eng. 93 (2003) 41–53.
[28] M. Haruta, M. Daté, Advances in the catalysis of Au nanoparticles, Appl. Cat. A. Gen. 22 (2001) 427–437.
[29] H.H. Kung, M.C. Kung, C.K. Costello, Supported Au catalysts for low temperature CO oxidation, J. Catal. 216 (2003) 425–432.
[30] M. Daté, M. Okumura, S. Tsubota, M. Haruta, Vital role of moisture in the catalytic activity of supported gold nanoparticles, Angew. Chem. Int. Ed. 43 (2004) 2129–2132.
[31] O.A. Simakova, B.T. Kusema, B.C. Campo, A.R. Leino, K. Kordás, V. Pitchon, P. Mäki-Arvela, D.Y. Murzin, Structure sensitivity in l-arabinose oxidation over Au/Al_2O_3 catalysts, J. Chem. Phys. 115 (2011) 1036–1043.
[32] E. Behravesh, K. Eränen, N. Kumar, J. Peltonen, M. Peurla, A. Aho, M. Nurmi, M. Toivakka, D.Y. Murzin, T. Salmi, Microreactor coating with Au/Al_2O_3 catalyst for gas-phase partial oxidation of ethanol: Physico-chemical characterization and evaluation of catalytic properties, J. Chem. Eng. 378 (2019).
[33] J. Enkovaara, C. Rostgaard, J.J. Mortensen, J. Chen, M. Dułak, L. Ferrighi, J. Gavnholt, C. Glinsvad, V. Haikola, H.A. Hansen, H.H. Kristoffersen, M. Kuisma, A.H. Larsen, L. Lehtovaara, M. Ljungberg, O. Lopez-Acevedo, P.G. Moses, J. Ojanen, T. Olsen, V. Petzold, N.A. Romero, J. Stausholm-Møller, M. Strange, G.A. Tritsaris, M. Vanin, M. Walter, B. Hammer, H. Häkkinen, G.K.H. Madsen, R.M. Nieminen, J.K. Nørskov, M. Puska, T.T. Rantala, J. Schiøtz, K.S. Thygesen, K.W. Jacobsen, Electronic structure calculations with GPAW: a real-space implementation of the projector augmented-wave method, J. Condens. Matter Phys. 22 (2010).
[34] J. Wellendorff, K.T. Lundgaard, A. Møgelhøj, V. Petzold, D.D. Landis, J. Nørskov, Density functionals for surface science: Exchange-correlation model development with Bayesian error estimation, Phys. Rev. B. Condens. Matter. Mater. Phys. 85 (2012).
[35] M. Dion, H. Rydberg, E. Schröder, D.C. Langreth, B.I. Lundqvist, Van der Waals density functional for general geometries, Phys. Rev. Lett. 92 (2005).
[36] G. Henkelman, H. Jónsson, Improved tangent estimate in the nudged elastic band method for finding minimum energy paths and saddle points, J. Phys. Chem. 113 (2000) 9978–9985.
[37] G. Henkelman, B.P. Uberuaga, H. Jónsson, A climbing image nudged elastic band method for finding saddle points and minimum energy paths, J. Phys. Chem. 113 (2000) 9901–9904.
[38] A. Hjorth Larsen, J. Jørgen Mortensen, J. Blomqvist, I.E. Castelli, R. Christensen, M. Dułak, J. Friis, M.N. Groves, B. Hammer, C. Hargus, E.D. Hermes, P.C. Jennings, P. Bjerre Jensen, J. Kermode, J.R. Kitchin, E. Leonhard Kolsbjerg, J. Kubal, K. Kaasbjerg, S. Lysgaard, J. Bergmann Maronsson, T. Maxson, T. Olsen, L. Pastewka, A. Peterson, C. Rostgaard, J. Schiøtz, O. Schütt, M. Strange, K.S. Thygesen, T. Vegge, L. Vilhelmsen, M. Walter, Z. Zeng, K.W. Jacobsen, The atomic simulation environment-a Python library for working with atoms, J Condens. Matter Phys. 29 (2017).
[39] E. Bitzek, P. Koskinen, F. Gähler, M. Moseler, P. Gumbsch, Structural Relaxation Made Simple, Phys. Rev. Lett. 97 (2006).
[40] R. Suerz, K. Eränen, N. Kumar, J. Wärnå, V. Russo, M. Peurla, A. Aho, D.Y. Murzin, T. Salmi, Application of microreactor technology to dehydration of bio-ethanol, Chem. Eng. Sci. 229 (2021).
[41] E. Behravesh, T. Kilpiö, V. Russo, K. Eränen, T. Salmi, Experimental and modelling study of partial oxidation of ethanol in a micro-reactor using gold nanoparticles as the catalyst, Chem. Eng. Sci. 176 (2018) 421–428.
[42] X. Yang, X. Wang, J. Qiu, Aerobic oxidation of alcohols over carbon nanotube-supported Ru catalysts assembled at the interfaces of emulsion droplets, Appl. Catal. A Gen. 382 (2010) 131–137.
[43] J. Gong, D.W. Flaherty, R.A. Ojifinni, J.M. White, C.B. Mullins, Surface chemistry of methanol on clean and atomic oxygen pre-covered Au (111), J. Chem. Phys. C 112 (2008) 5501–5509.
[44] J. Gong, C.B. Mullins, Selective oxidation of ethanol to acetaldehyde on gold, J. Am. Chem. Soc. 130 (2008) 16458–16459.
[45] J. Gong, D.W. Flaherty, T. Yan, C.B. Mullins, Selective oxidation of propanol on Au (111): Mechanistic insights into aerobic oxidation of alcohols, ChemPhysChem. 9 (2008) 2461–2466.
[46] T. Yan, J. Gong, C.B. Mullins, Oxygen exchange in the selective oxidation of 2-butanol on oxygen precovered Au (111), J. Am. Chem. Soc. 131 (2009) 16189–16194.
[47] R.L.H. Freire, D. Guedes-Sobrinho, A. Kiejna, J.L.F. da Silva, Comparison of the performance of van der Waals dispersion functionals in the description of water and ethanol on transition metal surfaces, J. Chem. Phys. C. 122 (2018) 1577–1588.
[48] Z.J. Zuo, L. Wang, P. Han, W. Huang, Effect of surface hydroxyls on dimethyl ether synthesis over the γ-Al_2O_3 in liquid paraffin: a computational study, J. Mol. Model. 19 (2013) 4959–4967.
[49] Z. Zuo, W. Huang, P. Han, Z. Gao, Z. Li, Theoretical studies on the reaction mechanisms of AlOOH- and γ-Al_2O_3-catalysed methanol dehydration in the gas and liquid phases, Appl. Catal. A Gen. 408 (2011) 130–136.
[50] M.A. Christiansen, G. Mpourmpakis, D.G. Vlachos, Density Functional Theory-computed mechanisms of ethylene and diethyl ether formation from ethanol on γ-Al_2O_3(100), ACS Catal. 3 (2013) 1965–1975.
[51] M.A. Christiansen, G. Mpourmpakis, D.G. Vlachos, DFT-driven multi-site microkinetic modeling of ethanol conversion to ethylene and diethyl ether on γ-Al_2O_3 (1 1 1), J. Catal. 323 (2015) 121–131.
[52] G.R. Jenness, M.A. Christiansen, S. Caratzoulas, D.G. Vlachos, R.J. Gorte, Site-dependent lewis acidity of γ-Al_2O_3 and its impact on ethanol dehydration and etherification, J. Chem. Phys. C 118 (2014) 12899–12907.
[53] K. Larmier, A. Nicolle, C. Chizallet, N. Cadran, S. Maury, A.F. Lamic-Humblot, E. Marceau, H. Lauron-Pernot, Influence of coadsorbed water and alcohol molecules on isopropyl alcohol dehydration on γ-alumina: Multiscale modeling of experimental kinetic profiles, ACS Catal. 6 (2016) 1905–1920.
[54] K. Larmier, C. Chizallet, N. Cadran, S. Maury, J. Abboud, A. Lamic-Humblot, E. Marceau, H. Lauron-Pernot, Mechanistic investigation of isopropanol

conversion on alumina catalysts: location of active sites for alkene/ether production, ACS Catal. 5 (2015) 4423–4437.
[55] E. Behravesh, N. Kumar, Q. Balme, J. Roine, J. Salonen, A. Schukarev, J.-P. Mikkola, M. Peurla, A. Aho, K. Eränen, D.Y. Murzin, T. Salmi, Synthesis and characterization of Au nano particles supported catalysts for partial oxidation of ethanol: Influence of solution pH, Au nanoparticle size, support structure and acidity, J. Catal. 353 (2017) 223–238.
[56] B. Xu, X. Liu, J. Haubrich, R.J. Madix, C.M. Friend, Selectivity control in gold-mediated esterification of methanol, Ang. Chem. Int. Eed. 48 (2009) 4206–4209.
[57] X. Liu, B. Xu, J. Haubrich, R.J. Madix, C.M. Friend, Surface-mediated self-coupling of ethanol on gold, J. Am. Chem. Soc. 131 (2009) 5757–5759.